Clinical Neurophysiology 169 (2025) 23–32

Contents lists available at ScienceDirect

Clinical Neurophysiology

journal homepage: www.elsevier.com/locate/clinph

Probing the orientation specificity of excitatory and inhibitory circuitries in the primary motor cortex with multi-channel TMS

Victor H. Souza [a,b,c,*], Jaakko O. Nieminen [a,b], Sergei Tugin [a,b], Lari M. Koponen [a,b,d,e], Ulf Ziemann [f,g], Oswaldo Baffa [c], Risto J. Ilmoniemi [a,b]

[a] Department of Neuroscience and Biomedical Engineering, Aalto University School of Science, Espoo, Finland
[b] BioMag Laboratory, HUS Medical Imaging Center, Aalto University, University of Helsinki and Helsinki University Hospital, Helsinki, Finland
[c] Department of Physics, Faculty of Philosophy, Sciences and Letters at Ribeirão Preto, University of São Paulo, Ribeirão Preto, Brazil
[d] Department of Psychiatry & Behavioral Sciences, Duke University, Durham, NC, USA
[e] Centre for Human Brain Health, School of Psychology, University of Birmingham, Birmingham, UK
[f] Department of Neurology & Stroke, University of Tübingen, Tübingen, Germany
[g] Hertie-Institute for Clinical Brain Research, University of Tübingen, Tübingen, Germany

ARTICLE INFO

Keywords:
Transcranial magnetic stimulation
Multi-locus TMS
Multi-channel TMS
Orientation sensitivity
Paired-pulse TMS
SICI
ICF
Inhibition
Facilitation
Motor evoked potential

ABSTRACT

Objective: Electric-field orientation is crucial for optimizing neuronal excitation in transcranial magnetic stimulation (TMS). Yet, the stimulus orientation effects on short-interval intracortical inhibition (SICI) and intracortical facilitation (ICF) are poorly understood due to technical challenges in manipulating the TMS-induced stimulus orientation within milliseconds. We aimed to assess the orientation sensitivity of SICI and ICF paradigms and identify optimal orientations for motor evoked potential (MEP) facilitation and suppression.
Methods: We applied paired-pulse multi-channel TMS to 12 healthy subjects with conditioning and test stimuli in the same, opposite, and perpendicular orientations to each other at four interstimulus intervals (ISI) to generate refractoriness, SICI, and ICF.
Results: MEP modulation was affected by the conditioning- and test-stimulus orientation, being strongest when both pulses were in the same direction. MEP modulation with 2.5-ms and 6.0-ms ISIs were more sensitive to orientation changes than 0.5- and 8.0-ms ISIs.
Conclusion: SICI and ICF orientation sensitivity exhibit a complex dependence on the conditioning stimulus orientation, which might be explained by anatomical and morphological arrangements of inhibitory and excitatory neuronal populations.
Significance: Distinct mechanisms mediating SICI and ICF are sensitive to stimulus orientation at specific ISIs, describing a structural–functional relationship that maximizes each effect at the cortical level.

1. Introduction

The inhibitory and excitatory neuronal circuits in the human neocortex modulate cortical excitation, which is critical for brain function. These neuronal circuits can be probed non-invasively in the human primary motor cortex through paired-pulse transcranial magnetic stimulation (TMS) (Chen, 2004). In paired-pulse TMS, a conditioning stimulus is followed by a test stimulus at a millisecond-range interval (Kujirai et al., 1993). Previous research demonstrated that fine adjustments of both stimuli parameters, such as interstimulus interval (ISI), pulse shape, current direction, and intensity, enable selective assessment of specific cortical circuitry (Cirillo et al., 2018; Fong et al., 2021; Hanajima et al., 1998; Hannah and Rothwell, 2017; Ilić et al., 2002; Nieminen et al., 2019; Ziemann et al., 1996). The parameter configuration in paired-pulse TMS ultimately defines the suppression or facilitation of motor evoked potential (MEP). Despite extensive research, to our knowledge, there is no comprehensive assessment of how specific combinations of conditioning and test stimulus orientations affect the excitatory and inhibitory circuits in the human primary motor cortex.

Suppression and facilitation of MEP responses are presumed to have separate neurophysiological origins for their distinct dependency on the stimulus parameters (for a review, see Di Lazzaro and Rothwell (Di Lazzaro and Rothwell, 2014)). The inhibitory effect seems to emerge from two different mechanisms depending on whether the ISI is shorter

* Corresponding author.
E-mail address: victor.souza@aalto.fi (V.H. Souza).

https://doi.org/10.1016/j.clinph.2024.11.004
Accepted 6 November 2024
Available online 16 November 2024

or longer than 1 ms. An ISI of 1 ms or shorter might inhibit the generation of descending volleys mainly by neuronal refractoriness due to the depolarization caused by a subthreshold conditioning stimulus (Fisher et al., 2002; Hanajima et al., 1998; Roshan et al., 2003). In turn, with ISIs between 1 and 5 ms, a short-interval intracortical inhibition (SICI) effect is dominated by transsynaptic release of gamma-aminobutyric acid A ($GABA_A$) (Di Lazzaro et al., 2000, 2006a,b; Mooney et al., 2017; Werhahn et al., 1999). With an ISI between 6 and 30 ms, motor responses are strengthened because of the intracortical facilitation (ICF) effect, presumably mediated by N-Methyl-D-aspartic acid (NMDA) (Chen, 2004; Schwenkreis et al., 1999; Ziemann et al., 1998).

The neuronal morphology coupled with the TMS-induced electric-field (E-field) orientation in the cortical tissue is a determinant factor for neural excitation (Bashir et al., 2013; Souza et al., 2022; Weise et al., 2023). Specific E-field orientations can selectively reach underlying mechanisms and neuronal populations associated with SICI and ICF phenomena (Fong et al., 2021; Hanajima et al., 1998; Tugin et al., 2021; Ziemann et al., 1996). For instance, MEP facilitation has been shown to vanish when the conditioning stimulus is rotated from being across to being along the central sulcus in ICF protocols (ISIs of 6–20 ms), whereas suppression of motor response is maintained in SICI protocols (ISIs of 1–4 ms) (Ziemann et al., 1996). In SICI with ISI of 1–3 ms, the level of MEP suppression depends on the direction of the conditioning stimulus. When both conditioning and test stimuli have the same direction for the TMS-induced current, the anterior–posterior direction has been shown to induce stronger inhibition than the posterior–anterior direction at rest (Cirillo et al., 2018; Cirillo and Byblow, 2016) and active muscles (Hanajima et al., 1998). In turn, for a fixed test stimulus in the posterior–anterior direction, an anterior–posterior conditioning stimulus resulted in weaker inhibition than a posterior–anterior conditioning stimulus (Fong et al., 2021) at rest but stronger inhibition with a slight muscle contraction (Hanajima et al., 1998). Still, the optimal combination of conditioning and test stimulus orientations that maximize refractoriness, SICI, and ICF remains unknown. Probing the orientation-sensitivity profile of these phenomena provides indirect evidence of the structural–functional relationship of neuronal circuits in the primary motor cortex by highlighting the anisotropic nature of the neuronal columnar organization and their directional sensitivities (Fox et al., 2004; Weise et al., 2023) coupled to the temporal dynamics of inhibitory and excitatory processes (Fisher et al., 2002; Hanajima et al., 1998; Ziemann et al., 1996).

Changing the TMS pulse orientation within millisecond intervals cannot be achieved by physical coil rotation, which has critically limited the scope of parameter configurations. Previous studies have tested mostly paired pulses in opposite directions (Cirillo and Byblow, 2016; Hanajima et al., 1998; Higashihara et al., 2020; Pavey et al., 2023). Others have superimposed two TMS coils to enable flexible adjustment of the cortically induced current direction (Fong et al., 2021; Ziemann et al., 1996), having limited control of the induced E-field spatial pattern, e.g., focality and accurate positioning, on the cortical surface. To solve these limitations, we recently developed the multi-channel TMS (mTMS) technology (Koponen et al., 2018a; Nieminen et al., 2022). The mTMS consists of an array of overlapping coils that enable precise control of the stimulus orientation at the desired ISI to study the intracortical mechanisms at the time scale of neuronal excitation (Nieminen et al., 2019; Souza et al., 2022; Tugin et al., 2021). With mTMS, we demonstrated that a conditioning stimulus delivered along the central sulcus (posterior–medial direction) induces stronger inhibition than a conditioning stimulus across the central sulcus (anterior–medial direction, i.e., posterior–anterior) (Tugin et al., 2021). Even with previous efforts, a comprehensive and systematic assessment of the SICI and ICF sensitivity to multiple test- and conditioning-stimulus orientations is still missing.

The aims of this study were: *i*) to leverage the flexible parameter control of mTMS to describe the orientation sensitivity of distinct mechanisms engaged in modulating the motor response through refractoriness (0.5-ms ISI), SICI (2.5-ms ISI), and ICF (6.0- and 8.0-ms ISI), and *ii*) to identify the optimal conditioning and test stimulus orientations that maximize the suppression and facilitation of MEPs. Our results support the future choice of stimulation parameters to selectively probe the cortical inhibitory and excitatory networks, being key for translating paired-pulse applications to data-driven automated cortical mapping paradigms (Tervo et al., 2022, 2020; Weise et al., 2020) and multi-channel TMS devices (Navarro de Lara et al., 2021; Nieminen et al., 2022).

2. Material and Methods

2.1. Participants

Twelve healthy volunteers (age: 29 years (mean), 27–41 years (range); 4 women; 8 right-handed (Oldfield, 1971)) participated in the study with a fully crossed and within-subject experimental design. All participants were free of neurological deficits and gave written informed consent before participation. The study was performed in accordance with the Declaration of Helsinki and approved by an Ethics Committee of the Hospital District of Helsinki and Uusimaa. Power analysis showed that with 11 participants, one can detect a mean difference in MEP amplitude of 0.125 mV with usual statistical significance ($\alpha = 0.05$) and power ($\beta = 0.20$). The sample size was calculated based on the framework proposed by (Ammann et al., 2020) and considering a Student's paired *t*-test (within-subject design; $r = 0.9$) with 20 MEP trials and *a posteriori* estimate from our recorded MEP amplitude standard deviation across trials ($\sigma_{\text{trials}} = 0.28$ mV) and between subjects ($\sigma_{\text{subjects}} = 0.26$ mV).

2.2. Experimental procedure

Data were recorded in the same experimental sessions reported for another study (Souza et al., 2022), with shared subject preparation, motor mapping, and resting motor threshold (rMT) determination. Briefly, surface electromyography (EMG) electrodes were placed over the right abductor pollicis brevis (APB), abductor digiti minimi, and first dorsal interosseous muscles in a belly–tendon montage. EMG was recorded with a Nexstim eXimia EMG device (500-Hz low-pass filtering, 3000-Hz sampling frequency; Nexstim Plc). Stimulation was delivered with a 2-coil mTMS system capable of manipulating the induced E-field orientation electronically within millisecond intervals without physically moving the coils (Souza et al., 2022; Tugin et al., 2021), illustrated in Fig. 1A. The mTMS coil array was placed following the subject's cortical anatomy using a neuronavigation system (NBS 3.2, Nexstim Plc) and an individual anatomical magnetic resonance image with voxel dimensions less than or equal to 1 mm. The hotspot and optimal orientation to elicit maximal MEP amplitudes on the APB muscle were obtained with the E-field peak induced by the bottom coil being approximately perpendicular to the central sulcus and with the induced peak E-field being anteromedial (AM), shown in Fig. 1B, during the rising phase of the trapezoidal monophasic pulse. The rMT was measured for AM and PL stimulus orientations as the lowest stimulus intensity capable of evoking at least 10 out of 20 MEPs with a minimum peak-to-peak amplitude of 50 μV (Rossini et al., 2015).

We employed a paired-pulse mTMS paradigm with the conditioning and test stimulus intensities at 80 and 110% rMT of the corresponding AM and PL test stimulus orientation, respectively. The 80% rMT intensity for the conditioning stimuli was selected to obtain MEP suppression and facilitation as in previous studies (Fong et al., 2021; Ilić et al., 2002; Kujirai et al., 1993; Nieminen et al., 2019). The relatively low test stimulus intensity was selected to obtain focal stimulation and evoke responses from a restricted motor representation area (van de Ruit and Grey, 2016; Tardelli et al., 2022) with narrow orientation sensitivity (Souza et al., 2022). Converting rMT to active MT (Ma et al., 2023), our 110 % rMT corresponds, on average, to a 145% active MT, which has

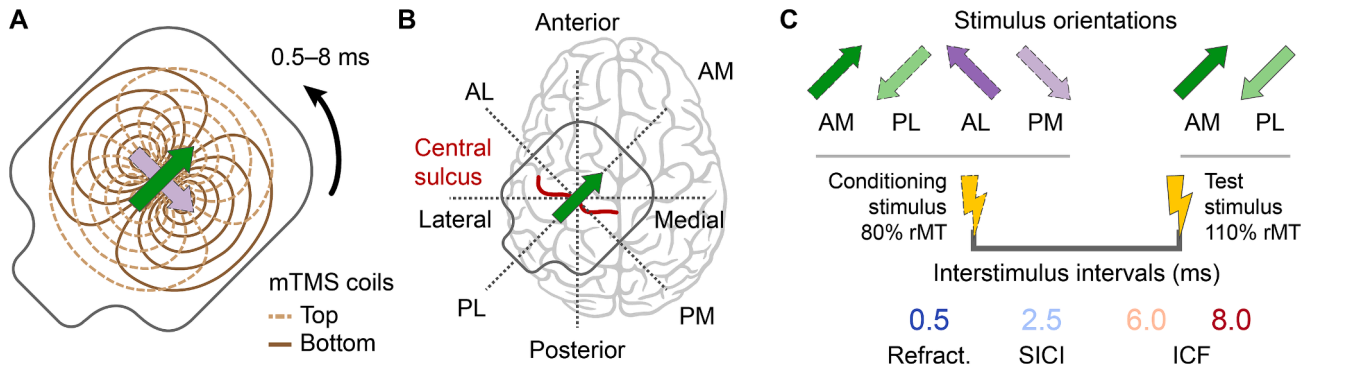

Fig. 1. Schematic representation of our experimental procedure. A) mTMS 2-coil wire paths with the bottom and top coils drawn in solid and dashed lines, respectively. The arrows above the coil wires represent the peak E-field induced by the conditioning and test stimulus, which can be electronically rotated at millisecond intervals. B) The peak induced E-field orientation relative to the central sulcus. The orientation labels indicate the current induced on the cortical surface by the rising phase of a trapezoidal monophasic waveform (described by Souza et al. (2022)). Current flows approximately perpendicular to the central sulcus on the anteromedial (AM) and posterolateral (PL) directions and along the central sulcus on posteromedial (PM) and anterolateral (AL) directions. C) The conditioning stimulus was delivered on AM, PL, AL, or PM orientations with an intensity of 80% of the resting motor threshold (rMT) at AM or PL (depending on the test stimulus). The test stimulus was delivered on AM or PL orientations at 110% of their corresponding rMT. Four interstimulus intervals (ISI) were employed to assess the following neurophysiological mechanisms: refractoriness (Refract.; 0.5 ms), short-interval intracortical inhibition (SICI; 2.5 ms), and intracortical facilitation (ICF; 6.0 and 8.0 ms).

been shown to evoke complete I-wave patterns in descending volleys (Di Lazzaro et al., 2001a), providing physiological mechanisms of SICI and ICF in a similar manner as at higher test stimulus intensities (Chen et al., 1998). We tested four ISIs (0.5, 2.5, 6, and 8 ms), four conditioning stimulus orientations (AM, posteromedial (PM), posterolateral (PL), and anterolateral (AL), and two test stimulus orientations (AM and PL). The 6-ms ISI is a transition towards ICF, while facilitation is stronger with an 8-ms ISI, which is also representative of longer ISIs (Ziemann et al., 1996). Therefore, we used 6- and 8-ms ISIs to identify whether they share similar TMS-induced orientation sensitivity, indicating similar underlying neurophysiological mechanisms.

The orientation terminology refers to the direction of the peak-induced E-field in the cortex (Fig. 1B). Twenty paired pulses were administered for each of the 32 combinations of conditioning and test stimulus orientations and ISI. An additional 20 single pulses (test stimulus alone) were applied in the AM and PL orientation at an intensity of 110% of their corresponding rMTs to record reference MEPs. In total, we recorded 680 trials per participant in a pseudo-randomized order with an intertrial interval pseudo-randomized from a uniform distribution between 4 to 6 s. Stimulation blocks lasted approximately 6 min and were separated by 2- to 5-minute breaks. Fig. 1C depicts all tested combinations of stimulus parameters.

The mTMS pulses had trapezoidal monophasic waveforms and were delivered by custom-made electronics (Koponen et al., 2018a, 2018b). The single-pulse stimulation intensity when determining the hotspot and the rMT was adjusted by varying the capacitor voltage with the current waveform phases lasting for 60.0 (rise), 30.0 (hold), and 43.2 μs (fall) (see (Souza et al., 2022) for a discussion on the orientation selectivity of trapezoidal and conventional monophasic TMS pulses). For the paired-pulse stimulation, the desired intensities were obtained by manipulating the duration of the rise, hold, and decay current waveform phases, as described by Nieminen et al. (2019) (see also (Peterchev et al., 2013; Shirota et al., 2016). The waveform durations were defined based on a model of neuronal depolarization during the mTMS pulses, accounting for the capacitor voltage drop due to the conditioning pulse and a reference neuronal membrane time constant of 200 μs (Barker et al., 1991; Koponen et al., 2018b). This approach allowed us to apply a pair of pulses at millisecond-scale intervals while producing the desired neuronal stimulation. The conditioning stimulus phase durations were 43.8, 30.0, and 32.5 μs, and the test stimulus phase durations were 75.1, 30.0, and 52.7 μs. mTMS current pulses and E-field waveforms are shown in Fig. 2. The temperature of the mTMS coil array enclosure was monitored with a thermal infrared camera (FLIR i3, FLIR Systems, USA). If the enclosure surface temperature reached 41 °C, it was cooled to about 30 °C.

2.3. Data analysis

Preprocessing: MEPs were extracted from the EMG recordings. Trials showing muscle pre-activation or movement artifacts greater than ±15 μV within 200 ms before the TMS pulse were removed from the analysis. For each trial, we computed the MEP peak-to-peak amplitude at 15–60 ms after the TMS pulse and manually annotated the MEP latency. The latencies from trials with a peak-to-peak amplitude below 50 μV were rejected from the analysis due to low signal-to-noise ratio and increased uncertainty in accurately defining the onset time. In total, 1.2% of the trials were rejected and 28.3% of the MEP latencies were not annotated. As expected, the relatively high amount of rejected latencies was due to the small MEPs in the SICI protocols (see Results below). For the single-pulse MEPs in AM and PL orientations, 11.4% and 31.9% of MEP latencies were not annotated. Even though the stimulation intensity at PL orientation was set based on its motor threshold, there was a higher number of trials with amplitudes below 50 μV, resulting in more latencies not being annotated. Data were pre-processed using custom-made scripts written in MATLAB R2021a (The MathWorks, Inc., USA).

Statistical analysis: The MEP amplitude and latency distributions were inspected visually for each subject and experimental condition to ensure a symmetric data distribution and similar variance across all conditions. The data of one subject were excluded from further analysis due to substantially small MEPs for all ISIs due to a high rMT, consistently deviating from the effects observed in all other participants. The MEP amplitudes were log-transformed to account for its skewed distribution associated with a relatively low test stimulus intensity (Goetz et al., 2014; Nielsen, 1996; Peterchev et al., 2013; Souza et al., 2024; Souza et al., 2022) and to correct for heteroskedasticity, i.e., variance inequalities across conditions. We analyzed and reported the raw MEP amplitude instead of ratios relative to the unconditioned amplitudes to account for the inherent variability of single-pulse MEPs (test stimulus alone) when estimating the inhibition and facilitation level (Souza et al., 2024; Tugin et al., 2021), which is otherwise disregarded and can bias the interpretation of effect sizes (Atchley et al., 1976; Jasienski and Bazzaz, 1999). The effect of the conditioning- and test-stimulus orientation and ISI on MEP amplitude and latency were assessed with linear mixed-effects models (Bates et al., 2015b; Yu et al., 2022). The model

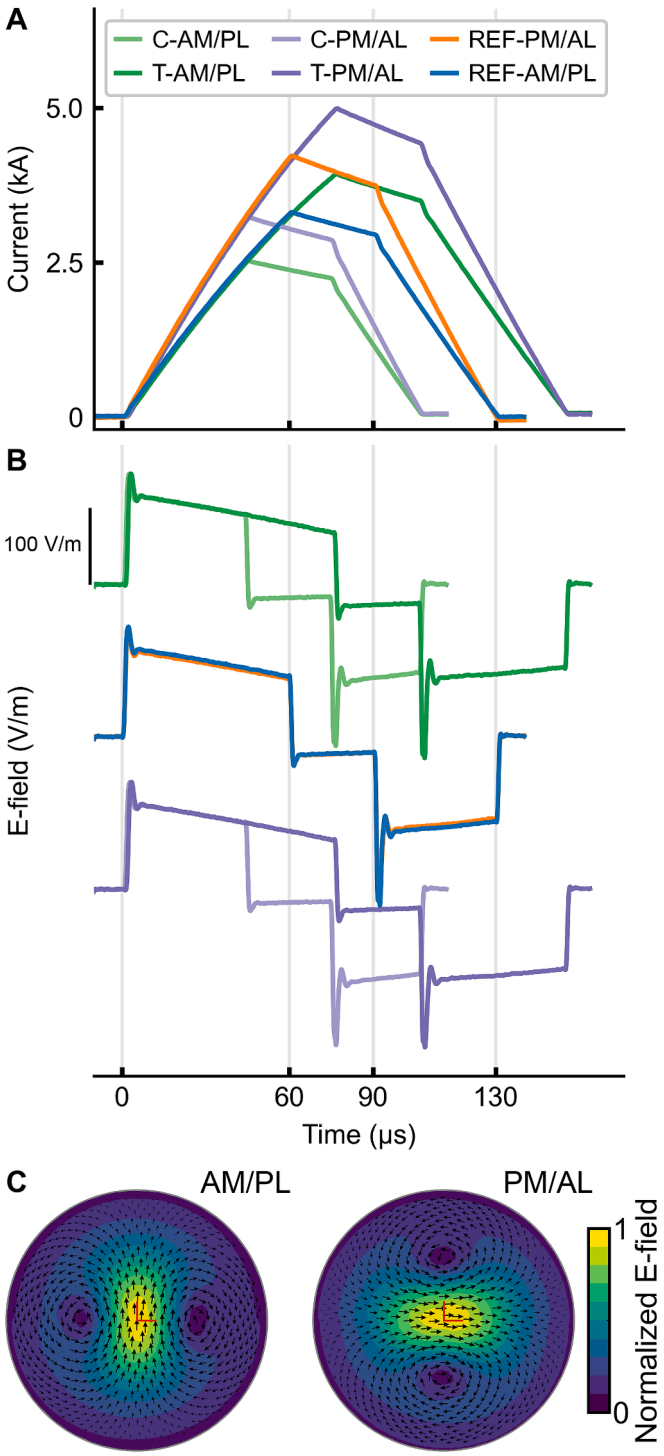

Fig. 2. mTMS current and e-field waveforms and spatial distributions. a) monophasic current waveform measured from bottom (green lines) and top (purple lines) coils with the pulse timings adjusted to induce an equivalent e-field at 80% (light lines) and 110% (dark lines) of resting motor threshold in paired-pulse paradigms without requiring changes to capacitor voltages. With the bottom coil, we delivered the conditioning (C-) and test (T-) stimuli in anteromedial (AM) and posterolateral (PL) orientations. With the top coil, we delivered the conditioning and test stimuli in anterolateral (AL) and posteromedial (PM) orientations. Because the top coil is further away from the cortex than the bottom, it requires a higher current to induce the same E-field intensity. The reference (REF-) waveforms (blue and orange lines) were used for single-pulse stimulation for hotspot and motor threshold determination with intensity set by adjusting the capacitor voltages, as in Ref. (Souza et al., 2022). B) Measured E-field waveforms with a 100-V/m average intensity during the rising part of the current corresponding to the current pulses in (A). All waveforms were lowpass filtered at 1 MHz. C) E-field spatial distribution for pulses given at AM, PL, PM or AL orientations (reproduced from (Souza et al., 2022)). E-fields were measured on a spherical surface with a 70-mm radius using our TMS characterizer (Nieminen et al., 2015). (For interpretation of the references to colour in this figure legend, the reader is referred to the web version of this article.)

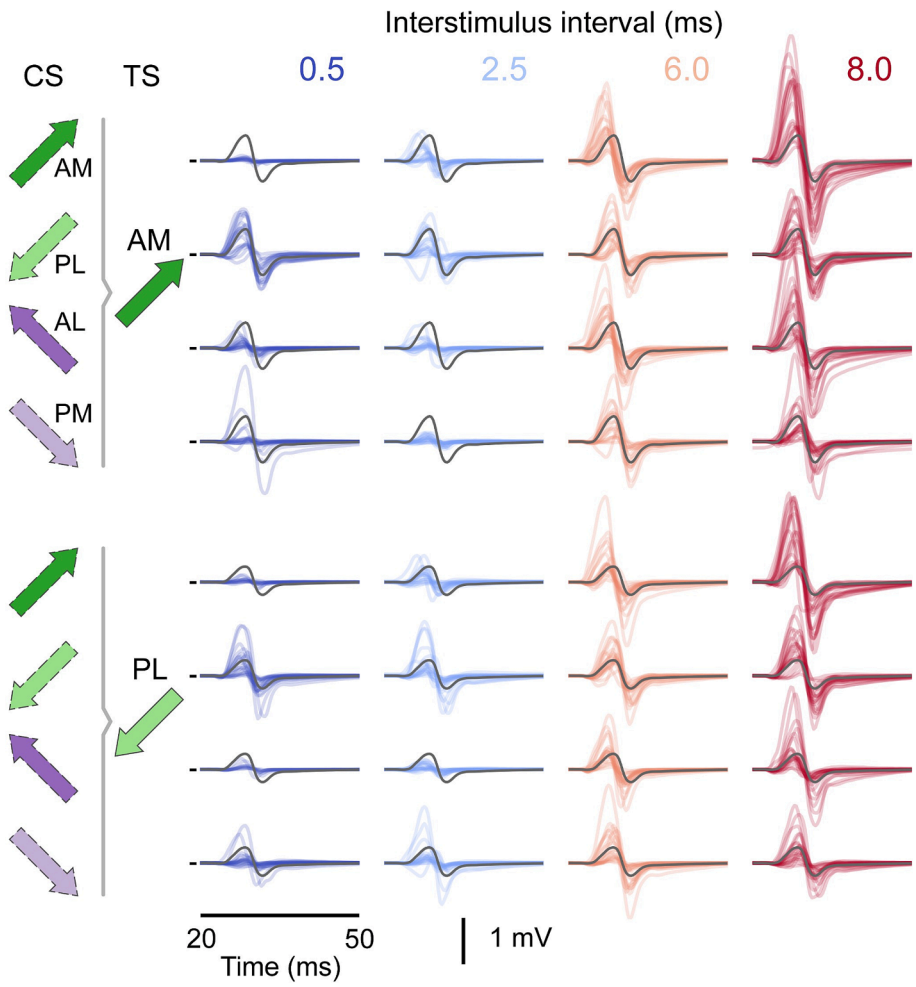

Fig. 3. Motor evoked potentials (MEP) of a representative subject from all tested conditions. The colored MEPs are single-trial recordings (non-averaged) from 20 to 50 ms after the TMS pulse at each combination of conditioning stimulus (CS) and test stimulus (TS) orientation and interstimulus interval (ISI). The gray solid traces represent the single-pulse MEPs averaged across 20 trials for each TS orientation. The single-pulse MEPs are replicated on all columns and rows of a given TS orientation for comparison with the corresponding paired-pulse MEPs. The arrow indicates the CS and TS orientation as in Fig. 1C. The TS was delivered in the anteromedial (AM) and posterolateral (PL) orientations, and the CS was delivered in the AM, posteromedial (PM), PL, and anterolateral (AL) orientations.

Table 1
Type III Analysis of Variance Table with Satterthwaite's method for the linear mixed-effects model of the MEP amplitude. Fixed factors were the test stimulus orientation (TS), conditioning stimulus orientation (CS), and interstimulus interval (ISI). Interaction between factors is represented as "×". The asterisk (*) indicates statistical significance ($p < 0.05$).

Effect	Degrees of freedom (numerator, denominator)	F-value	*p*-value
TS	(1, 10.0)	29.9	< 0.001*
CS	(3, 10.0)	5.1	0.02*
ISI	(3, 6846.3)	946.7	< 0.001*
TS × CS	(3, 6846.3)	22.6	< 0.001*
TS × ISI	(3, 6846.2)	2.6	0.05
CS × ISI	(9, 6846.3)	42.9	< 0.001*
TS × CS × ISI	(9, 6846.2)	8.4	< 0.001*

Table 2
Type III Analysis of Variance Table with Satterthwaite's method for the linear mixed-effects model of MEP latency. Fixed factors were the test stimulus orientation (TS), conditioning stimulus orientation (CS), and interstimulus interval (ISI). Interaction between factors is represented as "×". The asterisk (*) indicates statistical significance ($p < 0.05$).

Effect	Degrees of freedom (numerator, denominator)	F-value	*p*-value
TS	(1, 11.3)	24.0	< 0.001*
CS	(3, 10.6)	19.8	< 0.001*
ISI	(3, 3771.6)	55.8	< 0.001*
TS × CS	(3, 3703.5)	8.2	< 0.001*
TS × ISI	(3, 3650.2)	2.8	0.04*
CS × ISI	(9, 3363.2)	14.4	< 0.001*
TS × CS × ISI	(9, 3766.1)	1.3	0.21

comprised each condition and all possible interactions as fixed effects and a random structure with subject identifiers and correlated random intercepts and slopes for conditioning and test stimuli orientations. The random structure was selected based on sequential testing of hierarchical modeling with each model fit using likelihood-ratio tests (Barr et al., 2013; Bates et al., 2015a). A separate linear mixed-effects model was computed for quantifying facilitation and inhibition by

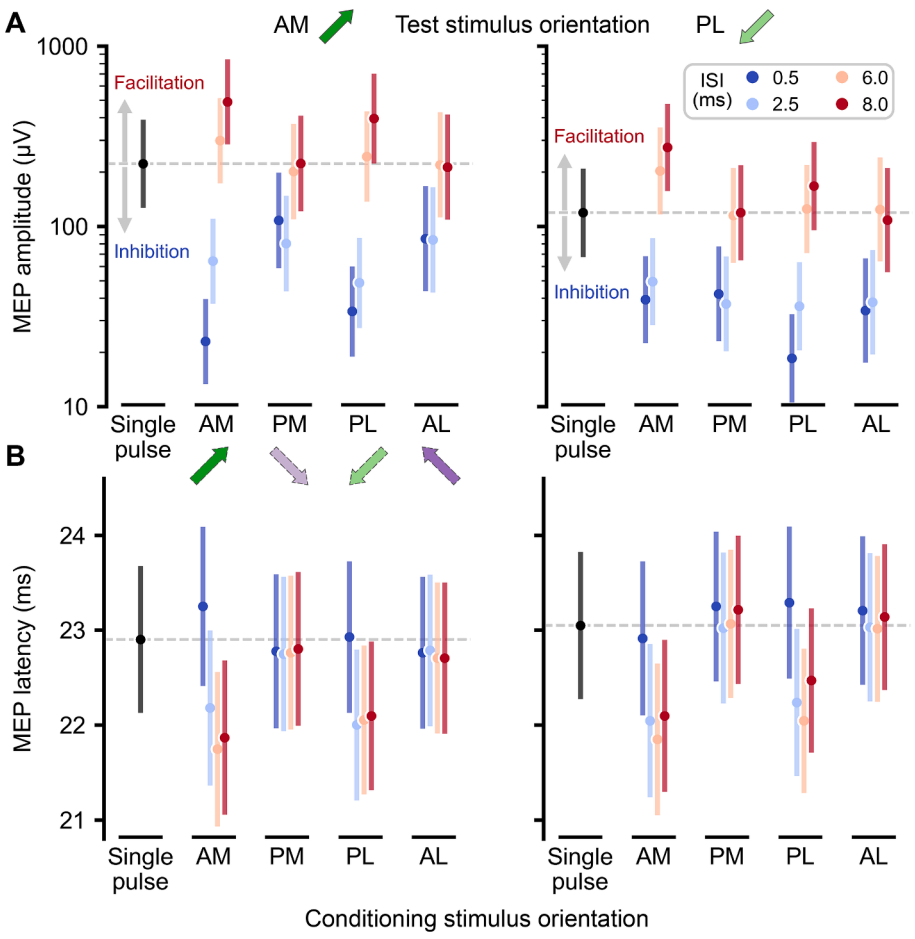

Fig. 4. Effect of stimulus orientation on refractoriness, SICI, and ICF. (**A**) MEP amplitude and (**B**) latency as a function of the conditioning stimulus orientation and interstimulus interval (ISI) for the test stimulus in the anteromedial (AM, left) and posterolateral (PL, right) orientations. The conditioning stimuli were delivered in the AM, posteromedial (PM), PL, and anterolateral (AL) orientations. The circular symbols mark the MEP amplitude or latency estimated by the linear mixed-effects model, and the vertical bars indicate the corresponding 95% confidence interval of the mean. The horizontal dashed gray line indicates the single-pulse MEP amplitude (**A**) or latency (**B**) in the model. The green and purple arrows refer to the stimulus orientations described in Fig. 1. (For interpretation of the references to colour in this figure legend, the reader is referred to the web version of this article.)

comparing all paired-pulse mTMS conditions with the corresponding MEPs from the test pulse alone, i.e., a single pulse. In this model, the fixed effects were the test stimulus orientation and all levels in paired-pulse mTMS (conditioning stimulus orientation and ISI) grouped to achieve a balanced design. The random structure of the paired- and single-pulse model had only the subject identifiers to account for varying MEP amplitude and latency intercepts. The selected models were recomputed using restricted maximum likelihood estimation and *p*-values for fixed-effects derived with Satterthwaite approximations in a Type III Analysis of Variance table. Post-hoc multiple comparisons were computed with estimated marginal means and *p*-values corrected for false discovery rate (Benjamini and Yekutieli, 2001). The model diagnostic was performed with Q–Q plots of residuals to assess any critical deviation from the normal distribution and standard versus fitted values plots to inspect for heteroscedasticity. Statistical analysis was performed using custom-made scripts written in R 4.3 (R Core Team, Vienna, Austria) with the *lme4* 1.1.35 and *afex* 1.3 packages for computing the linear mixed-effects models, and *emmeans* 1.10 for computing the estimated marginal means. The level of statistical significance was set to 0.05.

3. Results

The effects of test and conditioning stimulus orientation and ISI on the MEP traces of a representative subject are illustrated in Fig. 3. A single pulse in the PL orientation induced an MEP amplitude that was almost half of that observed with the test pulse in the AM orientation (standard error = 0.53, degrees-of-freedom = 12.2, *t*-ratio = −5.5, $p < 0.001$), with similar latencies at about 23 ms (standard error = 0.1, degrees-of-freedom = 9.8, *t*-ratio = 1.3, $p = 0.3$). The MEP amplitude inhibition and facilitation were significantly affected by changes in the test and conditioning stimulus orientation and ISI, as suggested by the significant interaction term (TS × CS × ISI) in Table 1. The MEP latency also varied depending on the pulse orientations, indicated by the significant interactions terms TS × CS and CS × ISI in Table 2. **Supplementary Tables S1–8** show all multiple comparison statistics for MEP amplitude and latency.

3.1. Effect of stimulus orientation on SICI

We observed different levels of MEP suppression depending on the conditioning and test stimulus orientation at 0.5- and 2.5-ms ISIs (Fig. 4A). For the 0.5-ms ISI, the strongest MEP inhibition (smallest amplitudes) occurred when the conditioning and test stimuli were applied in the AM orientation compared to the other orientations. Conditioning stimuli in the PM and AL orientations, i.e., perpendicular to the test stimulus, generated considerably less MEP suppression (higher amplitudes) than conditioning pulses in the AM and PL orientations. For instance, an AM conditioning stimulus orientation resulted in MEP amplitudes with about 10% of the MEP amplitudes elicited by

the test stimulus alone. In turn, conditioning stimuli in PL, AL, and PM directions suppressed MEP amplitudes to about 15%, 49%, and 39% of the average amplitude with the test stimulus alone (for all comparisons, $p < 0.001$). The effect of conditioning stimulus orientation differed for the 2.5-ms and 0.5-ms ISI. For the 2.5-ms ISI, a PL conditioning pulse evoked the smallest MEP amplitudes (conditioning and test stimuli in opposite directions) compared with the AM and PM orientations; conditioning pulses in PL and AL orientations resulted in similar amplitudes. These changes in MEP suppression were less prominent with the test stimulus in the PL orientation. Interestingly, with a pair of pulses in AM–AM orientation, the latencies at 2.5, 6.0, and 8.0-ms ISIs were 0.8–1.2 ms shorter than with the test pulse alone. Conditioning stimuli in the PM or AL orientation yielded MEPs with similar latencies to single-pulse MEPs regardless of the ISI and the test stimulus orientation.

3.2. *Effect of stimulus orientation on ICF*

MEP facilitation was observed only when the test and conditioning stimuli were either in the same or opposite directions and vanished for the conditioning stimulus (Fig. 4A), inducing an E-field perpendicular to the test stimulus. With an 8.0-ms ISI, the conditioning and test stimuli in AM and PL orientations facilitated the MEP amplitude, whereas with a 6.0-ms ISI, only the AM-oriented conditioning stimulus resulted in facilitation. The shortest MEP latencies were obtained at 6.0- and 8.0-ms ISIs with the conditioning and test stimuli in the same or opposite directions. When the conditioning and test pulses were perpendicular to each other, there was no significant difference in latency compared to the latency of single-pulse MEP at any ISI (Fig. 4B).

4. Discussion

Our results provide evidence that cortical mechanisms involved in the suppression and facilitation of MEPs exhibit a complex dependence on the conditioning stimulus orientation, which might be explained by distinct mechanisms mediating suppression and facilitation of neuronal activity. We demonstrated that the level of MEP amplitude suppression following the SICI protocols depended on the conditioning stimulus orientation. Moreover, MEP potentiation occurred only when the conditioning stimulus was delivered in the same or opposite direction as the test stimulus.

We found that a subthreshold conditioning stimulus followed by a suprathreshold test stimulus, either 0.5 or 2.5 ms later, caused a suppression in MEP amplitude in all the tested conditioning stimulus orientations. With a 2.5-ms ISI, the MEP inhibition was strongest when both pulses were delivered in the same direction, in line with previous findings using 2–3-ms ISI at rest (Cirillo and Byblow, 2016; Fong et al., 2021) and only observed for posteriorly directed stimuli at slight muscle contraction (Hanajima et al., 1998). We observed for the first time that the MEP suppression generated with a 0.5-ms ISI was strongest when the conditioning and test stimuli were given in the same or opposite directions and slightly reduced when the conditioning stimulus was delivered at PM and AL orientations.

Reduction in MEP amplitude at sub-millisecond ISIs may originate from a combination of axonal refractoriness and activation of inhibitory neuronal populations in superficial layers. The conditioning stimulus may induce refractoriness in specific orientation-sensitive pyramidal neuron segments, in line with (Fisher et al., 2002). In this case, the subsequent test stimulus would be less effective in directly stimulating those sites. The significant increase in MEP latency further supports this locally reduced excitability state due to neuronal refractoriness observed at 0.5-ms ISI only when the conditioning and test stimuli were delivered in the same direction. Refractoriness has been suggested to account for MEP suppression at 1-ms ISI but not at ISIs longer than 2–3 ms, showing a conditioning stimulus directionality sensitivity similar to what we observed (Fong et al., 2021). In turn, evidence from epidural recordings suggests that refractoriness might not play a crucial role at 1-ms ISI due to the preserved presence of I1-waves (Di Lazzaro et al., 1998). In this case, the suppression of MEP amplitude and longer MEP latency are better explained by the absence of I2- to I4-waves, which hinders the temporal summation of descending volleys at the spinal motor neuron required for generating a visible MEP. An experimental verification that refractoriness is responsible for the MEP suppression at 0.5-ms ISI might require epidural recordings to detect possible descending volleys even when there are no MEPs. If refractoriness does not play a critical role, MEP suppression might be primarily mediated by the excitation of $GABA_A$-mediated inhibitory interneurons that project horizontally within layers 2/3 with a distributed arborization (Esser et al., 2005; Porter et al., 2000). Like the excitatory mechanisms, a set of neuronal projections running from layers 2/3 to layer 5 would be optimally activated by a conditioning stimulus in the AM or PL orientations and explain the lower inhibition observed when the conditioning stimulus was delivered in the AL or PM orientations with a 0.5-ms ISI (Fig. 3A). This preferential excitation of specific groups of interneurons effectively suppresses I3-waves, observed as a reduction in MEP amplitude from the surface EMG (Hanajima et al., 1998). However, it is unlikely that both mechanisms would co-exist because the refractoriness of inhibitory interneurons would prevent the release of inhibitory neurotransmitters.

MEP facilitation was mainly observed when the conditioning stimulus was in the AM orientation for 6.0- and 8.0-ms ISIs and both AM and PL test stimulus orientations. Such specificity possibly indicates that ICF is mediated by connections across layers within a cortical column and thus exhibits a higher sensitivity to changes in the induced E-field orientation in the cortical tissue. Indeed, excitatory neurons exhibit a preferential direction projecting from layers 2/3 to pyramidal neurons in layer 5 (Esser et al., 2005; Kaneko et al., 2000) and thus might not be excited by the conditioning pulses in the AL and PM orientations. The subthreshold conditioning pulse possibly activated the low-threshold, fast inhibitory interneurons that later (after about 5 ms) depressed (Rusu et al., 2014), leaving the cortical circuitry in an excited state. This mechanism may only occur at rest, considering that a slight muscle contraction suppresses the generation of I-waves and disrupts the facilitatory effect from posterior-oriented conditioning and test pulses (Hanajima et al., 1998). The increased cortical excitability for the conditioning AM and PL pulses might also explain the shorter MEP latencies for 6.0 ms and 8.0 ms compared to the single-pulse stimulation. The excitation of intralayer projections evidences a similar orientation-dependency to that of the single-pulse MEPs, in which a stimulus in the AM orientation induces significantly higher neuronal excitation than in the PL orientation, as reported above.

The longer 8.0-ms ISI potentiated the MEPs even for conditioning stimulus in the PL orientation. This observation differs from a previous report with slight muscle contractions (Hanajima et al., 1998), in which the contractions suppress I-waves and reduce the potentiation effect of the conditioning stimulus. At rest and compared to the 6-ms ISI effect, the additional delay might further reduce the existing GABA inhibition (Rusu et al., 2014), and thus allow stronger neuronal activation even with a stimulus in the suboptimal PL orientation. The origin of mechanisms underlying MEP facilitation on ICF protocols is a composition of cortical and subcortical mechanisms. The facilitation of spinal reflexes by the conditioning pulse alone may suggest that ICF has a component at a subcortical level (Wiegel et al., 2018). In turn, the modulation of TMS-evoked electroencephalography responses evidences the primary enrolment of cortical circuits (Cash et al., 2017) other than those producing the high-frequency I-waves (Di Lazzaro et al., 2018), as the facilitation of MEP amplitude is not accompanied by changes in the amplitude and number of descending volleys (Di Lazzaro et al., 2006b; Ni et al., 2011).

The induced E-field orientation and stimulus intensity are intrinsically linked; thus, the interplay between stimulus orientation and intensity on SICI and ICF should be carefully considered. In this study, we adjusted the stimulus intensity for all conditions relative to the

corresponding test stimulus orientation (AM or PL orientation rMT). If otherwise adjusted for each orientation, it would probably aid differently in distinguishing the underlying mechanisms, as the stimulus intensity also determines the level of the SICI and ICF effects (Fong et al., 2021; Kujirai et al., 1993; Tugin et al., 2021). In addition, we noticed that there was only a marginal difference between MEP latencies with single pulses in the AM and PL orientations (Fig. 4B) like in our previous mTMS study (Souza et al., 2022) and with a half-sine (Sommer et al., 2006) and near-rectangular pulse (Sommer et al., 2018). This contrasts with the 2–3-ms difference observed with a classic monophasic pulse (Sommer et al., 2006), which supports the notion of multiple descending volleys elicited with the PL stimulus. As indicated in (Souza et al., 2022), such difference seems to be associated with the relatively strong E-field during the brief falling part of our current waveform affecting the neuronal membrane depolarization (Bromm and Frankenhaeuser, 1968). The distinct neuronal effects from the trapezoidal monophasic waveform should be carefully considered when comparing our SICI and ICF to those with a traditional monophasic pulse with a longer-lasting but weaker E-field during the current decay.

An important consideration is that most previous studies determined the effect of stimulus orientation on SICI and ICF as ratios or percentages relative to unconditioned MEP, e.g., with test stimulus alone (Fong et al., 2021; Hanajima et al., 1998; Ziemann et al., 1996). Even though ratios can be easier to interpret at first glance, they disregard the true nature of the unconditioned MEPs with their corresponding uncertainty in statistical estimates (Atchley et al., 1976; Jasienski and Bazzaz, 1999; Nielsen, 1996). This issue poses a risk of claiming that a specific combination of conditioning and test stimulus orientations had a statistically significant inhibition because it was lower than the single reference value attributed to the unconditioned MEP, i.e., 1 or 100%, when in fact, a statistical comparison between two distributions would not be significant. Therefore, our analysis using raw, non-normalized, repeated measure analysis provides a statistically robust estimate of MEP changes relative to the baseline measure to demonstrate the dependence of SICI and ICF on the TMS-induced stimulus orientation with appropriate uncertainty (Yu et al., 2022).

In the clinical context, changes in SICI and ICF have been identified as potential markers for neurological diseases, such as chronic neuropathic pain (Lefaucheur et al., 2006), amyotrophic lateral sclerosis (Vucic et al., 2018) and Parkinson's disease (Ni et al., 2013) (for a comprehensive review, see (Vucic et al., 2023)). Therefore, adjusting the stimulus orientation to maximize SICI and ICF might improve the specificity in probing $GABA_A$- and NMDA-mediated intracortical circuits, presumably enhancing the diagnostic precision. Furthermore, our paired-pulse mTMS with flexible orientation control is more conveniently implemented as a clinical device than previous approaches of stacking traditional TMS coils (Hanajima et al., 1998; Ziemann et al., 1996).

Our findings should be carefully interpreted due to the following limitations. First, our sample size of only 11 participants limited statistical power to detect small differences in MEP amplitude between highly suppressed MEP amplitude. The limited statistical power can result in not detecting differences when they exist (type II error). Second, we used the relatively low test stimulus intensity of 110% rMT, which might have caused a higher response variability than higher intensities (Brown et al., 2017; Goetz et al., 2014; Spampinato et al., 2023). A higher test stimulus intensity would then increase statistical power while compromising spatial and orientation selectivity in cortical stimulation (Souza et al., 2022; Tardelli et al., 2022). Third, our conditioning stimulus intensity of 80% rMT corresponds, on average, to 105% active MT (Ma et al., 2023). A stimulus near the active MT may evoke distinct corticospinal activity depending on the stimulus orientation (Di Lazzaro et al., 2001a; Di Lazzaro et al., 2001b), hindering our interpretations of purely corticocortical excitation and inhibition. This probably explains the decrease in MEP latency by, on average, 1 ms when the conditioning stimulus was delivered in the AM and PL orientations (except at a 0.5-ms ISI) compared to the single-pulse MEPs (Figs. 3 and 4). Fourth, our waveform durations differed between the conditioning and test stimulus, possibly having distinct mechanisms of neuronal excitation that also vary depending on the stimulus orientation (Sommer et al., 2018).

In conclusion, our results suggest a direct and strong relation between the orientation sensitivity of intracortical mechanisms and MEP suppression and facilitation, demonstrating the optimal combination of stimuli orientation that maximizes each effect. This orientation sensitivity describes the structural and physiological principles of neuronal refractoriness, SICI, and ICF at the cortical level.

CRediT authorship contribution statement

Victor H. Souza: Conceptualization, Methodology, Software, Formal analysis, Investigation, Writing – original draft, Writing – review & editing, Visualization. **Jaakko O. Nieminen:** Conceptualization, Methodology, Software, Formal analysis, Investigation, Writing – review & editing, Visualization. **Sergei Tugin:** Formal analysis, Data curation, Investigation, Writing – review & editing. **Lari M. Koponen:** Conceptualization, Methodology, Software, Formal analysis, Writing – review & editing. **Ulf Ziemann:** Validation, Writing – review & editing, Funding acquisition. **Oswaldo Baffa:** Resources, Writing – review & editing, Supervision, Funding acquisition. **Risto J. Ilmoniemi:** Conceptualization, Methodology, Resources, Writing – review & editing, Supervision, Funding acquisition.

Declaration of competing interest

The authors declare the following financial interests/personal relationships which may be considered as potential competing interests: [JON, LMK, and RJI are inventors of patents for mTMS technology. VHS is an inventor of patent applications for mTMS and TMS technologies. JON, RJI, and VHS have received unrelated consulting fees from Nexstim Plc. UZ received consulting fees from CorTec GmbH. The other authors declare no conflict of interest].

Acknowledgments

This study has received funding from the Research Council of Finland (Decisions No. 255347, 265680, 294625, 306845, and 349985), the Finnish Cultural Foundation, Jane and Aatos Erkko Foundation, Erasmus Mundus SMART2 (No. 552042-EM-1-2014-1-FR-ERA MUNDUSEMA2), the Conselho Nacional de Desenvolvimento Científico e Tecnológico (CNPq; grant number 140787/2014-3 and 305827/2023-5), the European Research Council (ERC) under the European Union's Horizon 2020 research and innovation programme (ConnectToBrain, grant agreement No 810377), and the Research, Innovation and Dissemination Center for Neuromathematics (FAPESP; grant number 2013/07699-0). We thank Heikki Sinisalo for assistance with the waveform measurements, the Aalto University Science-IT project for providing computational resources, and the Aalto NeuroImaging for its MRI facilities.

Appendix A. Supplementary data

Supplementary data to this article can be found online at https://doi.org/10.1016/j.clinph.2024.11.004.

References

Ammann, C., Guida, P., Caballero-Insaurriaga, J., Pineda-Pardo, J.A., Oliviero, A., Foffani, G., 2020. A framework to assess the impact of number of trials on the amplitude of motor evoked potentials. Sci. Rep. 10, 1–15. https://doi.org/10.1038/s41598-020-77383-6.

Atchley, W.R., Gaskins, C.T., Anderson, D., 1976. Statistical properties of ratios. I. Empirical Results. Syst. Zool. 25, 137. https://doi.org/10.2307/2412740.

Barker, A.T., Garnham, C.W., Freeston, I.L., 1991. Magnetic nerve stimulation: the effect of waveform on efficiency, determination of neural membrane time constants and the measurement of stimulator output. Electroencephalogr. Clin. Neurophysiol. Suppl. 43, 227–237.
Barr, D.J., Levy, R., Scheepers, C., Tily, H.J., 2013. Random effects structure for confirmatory hypothesis testing: Keep it maximal. J. Mem. Lang. 68, 255–278. https://doi.org/10.1016/j.jml.2012.11.001.
Bashir, S., Perez, J.M., Horvath, J.C., Pascual-Leone, A., 2013. Differentiation of motor cortical representation of hand muscles by navigated mapping of optimal TMS current directions in healthy subjects. J. Clin. Neurophysiol. 30, 390–395. https://doi.org/10.1097/WNP.0b013e31829dda6b.
Bates D, Kliegl R, Vasishth S, Baayen H. Parsimonious mixed models 2015a.
Bates, D., Mächler, M., Bolker, B., Walker, S., 2015b. Fitting linear mixed-effects models using lme4. J. Stat. Softw. 67. https://doi.org/10.18637/jss.v067.i01.
Benjamini, Y., Yekutieli, D., 2001. The control of the false discovery rate in multiple testing under dependency. Ann. Stat. 29, 1165–1188.
Bromm, B., Frankenhaeuser, B., 1968. Numerical calculation of the response in the myelinated nerve to short symmetrical double pulses. Pflügers Arch Gesamte Physiol Menschen Tiere 299, 357–363. https://doi.org/10.1007/BF00602911.
Brown, K.E., Lohse, K.R., Mayer, I.M.S., Strigaro, G., Desikan, M., Casula, E.P., et al., 2017. The reliability of commonly used electrophysiology measures. Brain Stimul. 10, 1102–1111. https://doi.org/10.1016/j.brs.2017.07.011.
Cash, R.F.H., Noda, Y., Zomorrodi, R., Radhu, N., Farzan, F., Rajji, T.K., et al., 2017. Characterization of glutamatergic and GABAA-mediated neurotransmission in motor and dorsolateral prefrontal cortex using paired-pulse TMS–EEG. Neuropsychopharmacology 42, 502–511. https://doi.org/10.1038/npp.2016.133.
Chen, R., 2004. Interactions between inhibitory and excitatory circuits in the human motor cortex. Exp. Brain Res. 154, 1–10. https://doi.org/10.1007/s00221-003-1684-1.
Chen, R., Tam, A., Bütefisch, C., Corwell, B., Ziemann, U., Rothwell, J.C., et al., 1998. Intracortical inhibition and facilitation in different representations of the human motor cortex. J. Neurophysiol. 80, 2870–2881. https://doi.org/10.1152/jn.1998.80.6.2870.
Cirillo, J., Byblow, W.D., 2016. Threshold tracking primary motor cortex inhibition: the influence of current direction. Eur. J. Neurosci. 44, 2614–2621. https://doi.org/10.1111/ejn.13369.
Cirillo, J., Semmler, J.G., Mooney, R.A., Byblow, W.D., 2018. Conventional or threshold-hunting TMS? A tale of two SICIs. Brain Stimul. 11, 1296–1305. https://doi.org/10.1016/j.brs.2018.07.047.
Di Lazzaro, V., Oliviero, A., Mazzone, P., Insola, A., Pilato, F., Saturno, E., et al., 2001a. Comparison of descending volleys evoked by monophasic and biphasic magnetic stimulation of the motor cortex in conscious humans. Exp. Brain Res. 141, 121–127. https://doi.org/10.1007/s002210100863.
Di Lazzaro, V., Oliviero, A., Saturno, E., Pilato, F., Insola, A., Mazzone, P., et al., 2001b. The effect on corticospinal volleys of reversing the direction of current induced in the motor cortex by transcranial magnetic stimulation. Exp. Brain Res. 138, 268–273. https://doi.org/10.1007/s002210100722.
Di Lazzaro, V., Rothwell, J.C., 2014. Corticospinal activity evoked and modulated by non-invasive stimulation of the intact human motor cortex. J. Physiol. 592, 4115–4128. https://doi.org/10.1113/jphysiol.2014.274316.
Di Lazzaro, V., Pilato, F., Dileone, M., Ranieri, F., Ricci, V., Profice, P., et al., 2006a. GABA A receptor subtype specific enhancement of inhibition in human motor cortex. J. Physiol. 575, 721–726. https://doi.org/10.1113/jphysiol.2006.114694.
Di Lazzaro, V., Pilato, F., Oliviero, A., Dileone, M., Saturno, E., Mazzone, P., et al., 2006b. Origin of facilitation of motor-evoked potentials after paired magnetic stimulation: direct recording of epidural activity in conscious humans. J. Neurophysiol. 96, 1765–1771. https://doi.org/10.1152/jn.00360.2006.
Di Lazzaro, V., Restuccia, D., Oliviero, A., Profice, P., Ferrara, L., Insola, A., et al., 1998. Magnetic transcranial stimulation at intensities below active motor threshold activates intracortical inhibitory circuits. Exp. Brain Res. 119, 265–268. https://doi.org/10.1007/s002210050341.
Di Lazzaro, V., Oliviero, A., Meglio, M., Cioni, B., Tamburrini, G., Tonali, P., et al., 2000. Direct demonstration of the effect of lorazepam on the excitability of the human motor cortex. Clin. Neurophysiol. 111, 794–799. https://doi.org/10.1016/S1388-2457(99)00314-4.
Di Lazzaro, V., Rothwell, J., Capogna, M., 2018. Noninvasive stimulation of the human brain: activation of multiple cortical circuits. Neuroscientist 24, 246–260. https://doi.org/10.1177/1073858417717660.
Esser, S.K., Hill, S.L., Tononi, G., 2005. Modeling the effects of transcranial magnetic stimulation on cortical circuits. J. Neurophysiol. 94, 622–639. https://doi.org/10.1152/jn.01230.2004.
Fisher, R.J., Nakamura, Y., Bestmann, S., Rothwell, J.C., Bostock, H., 2002. Two phases of intracortical inhibition revealed by transcranial magnetic threshold tracking. Exp. Brain Res. 143, 240–248. https://doi.org/10.1007/s00221-001-0988-2.
Fong, P.-Y., Spampinato, D., Rocchi, L., Hannah, R., Teng, Y., Di Santo, A., et al., 2021. Two forms of short-interval intracortical inhibition in human motor cortex. Brain Stimul. 14, 1340–1352. https://doi.org/10.1016/j.brs.2021.08.022.
Fox, P.T., Narayana, S., Tandon, N., Sandoval, H., Fox, S.P., Kochunov, P., et al., 2004. Column-based model of electric field excitation of cerebral cortex. Hum. Brain Mapp. 22, 1–14. https://doi.org/10.1002/hbm.20006.
Goetz, S.M., Luber, B., Lisanby, S.H., Peterchev, A.V., 2014. A novel model incorporating two variability sources for describing motor evoked potentials. Brain Stimul. 7, 541–552. https://doi.org/10.1016/j.brs.2014.03.002.
Hanajima, R., Ugawa, Y., Terao, Y., Sakai, K., Furubayashi, T., Machii, K., et al., 1998. Paired-pulse magnetic stimulation of the human motor cortex: differences among I waves. J. Physiol. 509, 607–618. https://doi.org/10.1111/j.1469-7793.1998.607bn.x.
Hannah, R., Rothwell, J.C., 2017. Pulse duration as well as current direction determines the specificity of transcranial magnetic stimulation of motor cortex during contraction. Brain Stimul. 10, 106–115. https://doi.org/10.1016/j.brs.2016.09.008.
Higashihara, M., Van den Bos, M.A.J., Menon, P., Kiernan, M.C., Vucic, S., 2020. Interneuronal networks mediate cortical inhibition and facilitation. Clin. Neurophysiol. 131, 1000–1010. https://doi.org/10.1016/j.clinph.2020.02.012.
Ilić, T.V., Meintzschel, F., Cleff, U., Ruge, D., Kessler, K.R., Ziemann, U., 2002. Short-interval paired-pulse inhibition and facilitation of human motor cortex: the dimension of stimulus intensity. J. Physiol. 545, 153–167. https://doi.org/10.1113/jphysiol.2002.030122.
Jasienski, M., Bazzaz, F.A., 1999. The fallacy of ratios and the testability of models in biology. Oikos 84, 321. https://doi.org/10.2307/3546729.
Kaneko, T., Cho, R.-H., Li, Y.-Q., Nomura, S., Mizuno, N., 2000. Predominant information transfer from layer III pyramidal neurons to corticospinal neurons. J. Comp. Neurol. 423, 52–65. https://doi.org/10.1002/1096-9861(20000717)423:1<52::AID-CNE5>3.0.CO;2-F.
Koponen, L.M., Nieminen, J.O., Ilmoniemi, R.J., 2018a. Multi-locus transcranial magnetic stimulation—theory and implementation. Brain Stimul. 11, 849–855. https://doi.org/10.1016/j.brs.2018.03.014.
Koponen, L.M., Nieminen, J.O., Mutanen, T.P., Ilmoniemi, R.J., 2018b. Noninvasive extraction of microsecond-scale dynamics from human motor cortex. Hum. Brain Mapp. 39, 2405–2411. https://doi.org/10.1002/hbm.24010.
Kujirai, T., Caramia, M.D., Rothwell, J.C., Day, B.L., Thompson, P.D., Ferbert, A., et al., 1993. Corticocortical inhibition in human motor cortex. J. Physiol. 471, 501–519. https://doi.org/10.1113/jphysiol.1993.sp019912.
Lefaucheur, J.P., Drouot, X., Ménard-Lefaucheur, I., Keravel, Y., Nguyen, J.P., 2006. Motor cortex rTMS restores defective intracortical inhibition in chronic neuropathic pain. Neurology 67, 1568–1574. https://doi.org/10.1212/01.WNL.0000242731.10074.3C.
Ma, K., Hamada, M., Di Lazzaro, V., Hand, B., Guerra, A., Opie, G.M., et al., 2023. Correlating active and resting motor thresholds for transcranial magnetic stimulation through a matching model. Brain Stimul. 16, 1686–1688. https://doi.org/10.1016/j.brs.2023.11.009.
Mooney, R.A., Cirillo, J., Byblow, W.D., 2017. GABA and primary motor cortex inhibition in young and older adults: a multimodal reliability study. J. Neurophysiol. 118, 425–433. https://doi.org/10.1152/jn.00199.2017.
Navarro de Lara, L.I., Daneshzand, M., Mascarenas, A., Paulson, D., Pratt, K., Okada, Y., et al., 2021. A 3-axis coil design for multichannel TMS arrays. Neuroimage 224, 117355. https://doi.org/10.1016/j.neuroimage.2020.117355.
Ni, Z., Gunraj, C., Wagle-Shukla, A., Udupa, K., Mazzella, F., Lozano, A.M., et al., 2011. Direct demonstration of inhibitory interactions between long interval intracortical inhibition and short interval intracortical inhibition. J. Physiol. 589, 2955–2962. https://doi.org/10.1113/jphysiol.2011.207928.
Ni, Z., Bahl, N., Gunraj, C.A., Mazzella, F., Chen, R., 2013. Increased motor cortical facilitation and decreased inhibition in Parkinson disease. Neurology 80, 1746–1753. https://doi.org/10.1212/WNL.0b013e3182919029.
Nielsen, J.F., 1996. Logarithmic distribution of amplitudes of compound muscle action potentials evoked by transcranial magnetic stimulation. J. Clin. Neurophysiol. 13, 423–434. https://doi.org/10.1097/00004691-199609000-00005.
Nieminen, J.O., Koponen, L.M., Ilmoniemi, R.J., 2015. Experimental characterization of the electric field distribution induced by TMS devices. Brain Stimul. 8, 582–589. https://doi.org/10.1016/j.brs.2015.01.004.
Nieminen, J.O., Koponen, L.M., Mäkelä, N., Souza, V.H., Stenroos, M., Ilmoniemi, R.J., 2019. Short-interval intracortical inhibition in human primary motor cortex: a multi-locus transcranial magnetic stimulation study. Neuroimage 203, 116194. https://doi.org/10.1016/j.neuroimage.2019.116194.
Nieminen, J.O., Sinisalo, H., Souza, V.H., Malmi, M., Yuryev, M., Tervo, A.E., et al., 2022. Multi-locus transcranial magnetic stimulation system for electronically targeted brain stimulation. Brain Stimul. 15, 116–124. https://doi.org/10.1016/j.brs.2021.11.014.
Oldfield, R.C., 1971. The assessment and analysis of handedness: the Edinburgh inventory. Neuropsychologia 9, 97–113. https://doi.org/10.1016/0028-3932(71)90067-4.
Pavey, N., Menon, P., van den Bos, M.A.J., Kiernan, M.C., Vucic, S., 2023. Cortical inhibition and facilitation are mediated by distinct physiological processes. Neurosci. Lett. 803, 137191. https://doi.org/10.1016/j.neulet.2023.137191.
Peterchev, A.V., Goetz, S.M., Westin, G.G., Luber, B., Lisanby, S.H., 2013. Pulse width dependence of motor threshold and input–output curve characterized with controllable pulse parameter transcranial magnetic stimulation. Clin. Neurophysiol. 124, 1364–1372. https://doi.org/10.1016/j.clinph.2013.01.011.
Porter, L.L., Matin, D., Keller, A., 2000. Characteristics of GABAergic neurons and their synaptic relationships with intrinsic axons in the cat motor cortex. Somatosens Mot. Res. 17, 67–80. https://doi.org/10.1080/08990220070319.
Roshan, L., Paradiso, G.O., Chen, R., 2003. Two phases of short-interval intracortical inhibition. Exp. Brain Res. 151, 330–337. https://doi.org/10.1007/s00221-003-1502-9.
Rossini, P.M., Burke, D., Chen, R., Cohen, L.G., Daskalakis, Z., Di Iorio, R., et al., 2015. Non-invasive electrical and magnetic stimulation of the brain, spinal cord, roots and peripheral nerves: Basic principles and procedures for routine clinical and research application. An updated report from an I.F.C.N. Committee. Clin. Neurophysiol. 126, 1071–1107. https://doi.org/10.1016/j.clinph.2015.02.001.
Rusu, C.V., Murakami, M., Ziemann, U., Triesch, J., 2014. A model of TMS-induced I-waves in motor cortex. Brain Stimul. 7, 401–414. https://doi.org/10.1016/j.brs.2014.02.009.

Schwenkreis, P., Witscher, K., Janssen, F., Addo, A., Dertwinkel, R., Zenz, M., et al., 1999. Influence of the N-methyl-d-aspartate antagonist memantine on human motor cortex excitability. Neurosci. Lett. 270, 137–140. https://doi.org/10.1016/S0304-3940(99)00492-9.

Shirota, Y., Sommer, M., Paulus, W., 2016. Strength-duration relationship in paired-pulse transcranial magnetic stimulation (TMS) and its implications for repetitive TMS. Brain Stimul. 9, 755–761. https://doi.org/10.1016/j.brs.2016.04.019.

Sommer, M., Alfaro, A., Rummel, M., Speck, S., Lang, N., Tings, T., et al., 2006. Half sine, monophasic and biphasic transcranial magnetic stimulation of the human motor cortex. Clin. Neurophysiol. 117, 838–844. https://doi.org/10.1016/j.clinph.2005.10.029.

Sommer, M., Ciocca, M., Chieffo, R., Hammond, P., Neef, A., Paulus, W., et al., 2018. TMS of primary motor cortex with a biphasic pulse activates two independent sets of excitable neurones. Brain Stimul. 11, 558–565. https://doi.org/10.1016/j.brs.2018.01.001.

Souza, V.H., Nieminen, J.O., Tugin, S., Koponen, L.M., Baffa, O., Ilmoniemi, R.J., 2022. TMS with fast and accurate electronic control: Measuring the orientation sensitivity of corticomotor pathways. Brain Stimul. 15, 306–315. https://doi.org/10.1016/j.brs.2022.01.009.

Souza, V.H., Villa-Flor de Castro, K., de Melo-Carneiro, P., de Oliveira, G.I., Ribeiro Camatti, J., Adélia Victor Fernandes de Oliveira, I., et al., 2024. tDCS and local scalp cooling do not change corticomotor and intracortical excitability in healthy humans. Clin. Neurophysiol. https://doi.org/10.1016/j.clinph.2024.09.023.

Spampinato, D., Ibanez, J., Rocchi, L., Rothwell, J., 2023. Motor potentials evoked by transcranial magnetic stimulation: interpreting a simple measure of a complex system. J. Physiol. 601, 2827–2851. https://doi.org/10.1113/JP281885.

Tardelli, G.P., Souza, V.H., Matsuda, R.H., Garcia, M.A.C., Novikov, P.A., Nazarova, M. A., et al., 2022. Forearm and hand muscles exhibit high coactivation and overlapping of cortical motor representations. Brain Topogr. 35, 322–336. https://doi.org/10.1007/s10548-022-00893-1.

Tervo, A.E., Metsomaa, J., Nieminen, J.O., Sarvas, J., Ilmoniemi, R.J., 2020. Automated search of stimulation targets with closed-loop transcranial magnetic stimulation. Neuroimage 220, 117082. https://doi.org/10.1016/j.neuroimage.2020.117082.

Tervo, A.E., Nieminen, J.O., Lioumis, P., Metsomaa, J., Souza, V.H., Sinisalo, H., et al., 2022. Closed-loop optimization of transcranial magnetic stimulation with electroencephalography feedback. Brain Stimul. 15, 523–531. https://doi.org/10.1016/j.brs.2022.01.016.

Tugin, S., Souza, V.H., Nazarova, M.A., Novikov, P.A., Tervo, A.E., Nieminen, J.O., et al., 2021. Effect of stimulus orientation and intensity on short-interval intracortical inhibition (SICI) and facilitation (SICF): a multi-channel transcranial magnetic stimulation study. PLoS One 16, e0257554. https://doi.org/10.1371/journal.pone.0257554.

van de Ruit, M., Grey, M.J., 2016. The TMS map scales with increased stimulation intensity and muscle activation. Brain Topogr. 29, 56–66. https://doi.org/10.1007/s10548-015-0447-1.

Vucic, S., van den Bos, M., Menon, P., Howells, J., Dharmadasa, T., Kiernan, M.C., 2018. Utility of threshold tracking transcranial magnetic stimulation in ALS. Clin. Neurophysiol. Pract. 3, 164–172. https://doi.org/10.1016/J.CNP.2018.10.002.

Vucic, S., Stanley Chen, K.-H., Kiernan, M.C., Hallett, M., DavidH, B., Di Lazzaro, V., et al., 2023. Clinical diagnostic utility of transcranial magnetic stimulation in neurological disorders. Updated report of an IFCN committee. Clin. Neurophysiol. 150, 131–175. https://doi.org/10.1016/j.clinph.2023.03.010.

Weise, K., Numssen, O., Thielscher, A., Hartwigsen, G., Knösche, T.R., 2020. A novel approach to localize cortical TMS effects. Neuroimage 209, 116486. https://doi.org/10.1016/j.neuroimage.2019.116486.

Weise, K., Worbs, T., Kalloch, B., Souza, V.H., Jaquier, A.T., Van Geit, W., et al., 2023. Directional sensitivity of cortical neurons towards TMS-induced electric fields. Imaging Neurosci. 1, 1–22. https://doi.org/10.1162/imag_a_00036.

Werhahn, K.J., Kunesch, E., Noachtar, S., Benecke, R., Classen, J., 1999. Differential effects on motorcortical inhibition induced by blockade of GABA uptake in humans. J. Physiol. 517, 591–597. https://doi.org/10.1111/j.1469-7793.1999.0591t.x.

Wiegel, P., Niemann, N., Rothwell, J.C., Leukel, C., 2018. Evidence for a subcortical contribution to intracortical facilitation. Eur. J. Neurosci. 47, 1311–1319. https://doi.org/10.1111/ejn.13934.

Yu, Z., Guindani, M., Grieco, S.F., Chen, L., Holmes, T.C., Xu, X., 2022. Beyond t test and ANOVA: applications of mixed-effects models for more rigorous statistical analysis in neuroscience research. Neuron 110, 21–35. https://doi.org/10.1016/j.neuron.2021.10.030.

Ziemann, U., Rothwell, J.C., Ridding, M.C., 1996. Interaction between intracortical inhibition and facilitation in human motor cortex. J. Physiol. 496, 873–881. https://doi.org/10.1113/jphysiol.1996.sp021734.

Ziemann, U., Chen, R., Cohen, L.G., Hallett, M., 1998. Dextromethorphan decreases the excitability of the human motor cortex. Neurology 51, 1320–1324. https://doi.org/10.1212/WNL.51.5.1320.